Optimized evaporative cooling for sodium Bose-Einstein condensation against three-body loss

Takahiko Shobu, Hironobu Yamaoka, Hiromitsu Imai, and Atsuo Morinaga
Department of Physics, Faculty of Science and Technology, Tokyo University of Science, Yamazaki, Noda-shi, Chiba 278-8510, Japan

Makoto Yamashita
NTT Basic Research Laboratories, NTT Corporation, 3-1 Morinosato-Wakamiya, Atsugi-shi, Kanagawa 243-0198, Japan and Japan Science and Technology Agency, CREST, 5, Sanbancho, Chiyoda-ku Tokyo 102-0075, Japan
(Received 24 February 2011; published 20 September 2011)

We report on a highly efficient evaporative cooling optimized experimentally. We successfully created sodium Bose-Einstein condensates with 6.4×10^7 atoms starting from 6.6×10^9 thermal atoms trapped in a magnetic trap by employing a fast linear sweep of radio frequency at the final stage of evaporative cooling so as to overcome the serious three-body losses. The experimental results such as the cooling trajectory and the condensate growth quantitatively agree with the numerical simulations of evaporative cooling on the basis of the kinetic theory of a Bose gas carefully taking into account our specific experimental conditions. We further discuss theoretically a possibility of producing large condensates, more than 10^8 sodium atoms, by simply increasing the number of initial thermal trapped atoms and the corresponding optimization of evaporative cooling.

DOI: 10.1103/PhysRevA.84.033626 PACS number(s): 03.75.Kk, 05.30.Jp, 37.10.De

I. INTRODUCTION

It has been 15 years since Bose-Einstein condensation (BEC) in an atomic vapor was first realized in a high-current magnetic trap [1,2]. Presently, BEC can be produced on an atom chip with thin wires [3] and in an optical trap [4] for a variety of scientific or technological purposes. The number of atoms in such BECs are 10^6 at most. On the other hand, BEC with a large number of atoms (more than 10^7 atoms) is necessary to develop a quasicontinuous atom laser [5] or an atom interferometer for precise measurement [6]. A large atom number allows better signal-to-noise ratios, greater tolerance against misalignments, and greater robustness in day-to-day operation. The key technology for creating BEC with a large atom number is the efficient evaporative cooling of atoms trapped in the high-current magnetic trap (MT). Evaporative cooling is at present the most powerful method of increasing the phase-space density of atoms $\rho = n\lambda_{\mathrm{dB}}^3$ from 10^{-6} at the magnetic trap to $\sim$1 to achieve BEC. The mechanism of the evaporative cooling is based on both the selective removal of energetic atoms through evaporation and collisional rethermalizations among the remaining atoms [7,8]. In rf-induced forced evaporative cooling, the magnetic trap height is determined by the applied rf-magnetic field (truncation energy), and cooling increases the density of atoms and the elastic collision rate, thereby accelerating evaporation. However, the method is also subject to undesirable losses, for example, loss caused by elastic collisions with the background gas, two-body dipolar relaxation, and three-body recombination [9]. Therefore, it is highly desirable to find the best way of rf sweep for the evaporative cooling with the highest speed and efficiency to create a large BEC, competing with the loss process. The sodium atom is suitable for creating a large BEC because the three-body loss is comparatively small. To date, the MIT group has produced sodium BEC with atom number of $(2\text{–}10)\times10^7$ [10] and the Utrecht University group produced the BEC with 1.2×10^8 sodium atoms [11]. The ratio of the number of atoms in BEC on the number of trapped atoms in the MT, that is, efficiency was 0.8%. The latter recently has succeeded in producing the largest sodium BEC with 3×10^8 atoms [12].

There are several theoretical models describing the evaporative cooling processes, including Monte Carlo simulation [13–15]. Yamashita *et al.* developed a method of calculating evaporative cooling based on the kinetic theory of a Bose gas and found that a fast sweep at the final stage of evaporative cooling is effective for producing a large number of condensates against the three-body recombination [16]. The fact was verified by the efficient production of 2×10^6 BEC in ^{87}Rb atom with an efficiency of 0.4% by Mukai and Yamashita [17]. Previously, the authors reported the creation of the sodium BEC with 1.5×10^6 atoms from 1.3×10^9 atoms trapped in the MT [18]. It took 90 s to reach phase transition and the efficiency was 0.12%. In this case, the cooling trajectory during evaporative cooling was not optimized. The density of sodium atoms was 1×10^{14} atoms/cm^3, so that there was no distinct difference between the fast and slow rf sweeps. The three-body loss rate of sodium atoms is one-eighth that of Rb atoms [19]. However, if we produce a sodium BEC with more than 1×10^7 atoms, the three-body loss also becomes a serious problem if the density is more than 2×10^{14} atoms/cm^3. Therefore, the MIT group [10] and the Utrecht University group [11] used decompression of the magnetic trap near the end of the evaporation process to produce a large BEC, by which the loss due to the three-body recombination was reduced and the final density of condensates decreased. However, it was noted that the decompression shifts the trap center due to gravitational sag and excites oscillations in the cloud of BEC [10].

In this paper we explore a method of efficient evaporative cooling of sodium atom experimentally and examine the effect of the fast sweep at the final evaporative stage to produce a large atom number sodium BEC. The measured cooling trajectory is found to be very close to the optimum one obtained by the kinetic theory of a Bose gas, which proves the significant high efficiency of our present evaporative cooling. In Sec. II we summarize the theoretical approach employed in the present study. We then in Sec. III present the experimental results of

our optimized evaporative cooling. In Sec IV we discuss the efficiency of our evaporative cooling and the serious influence of three-body loss on the growth of sodium condensates by quantitatively comparing between the experimental results and the theoretical simulations. Finally, the conclusions of this work are provided.

II. THEORETICAL METHOD

In this section we review the theoretical method based on the kinetic theory of a Bose gas used in this work. After a brief explanation of our theoretical framework [16] (Sec. II A), we show in Sec. II B quantitative numerical simulations corresponding to our previous experiments [18] and discuss the influence of three-body recombination loss on the growth of condensates in these experiments. In Sec. II C we mention the optimization of cooling trajectory to achieve the highly efficient evaporative cooling [19].

A. Kinetic theory of evaporative cooling

We begin by explaining the thermodynamics of trapped atoms. During evaporative cooling the magnetic trapping potential $U(\mathbf{r})$ is truncated at the energy that is determined by the frequency of the applied rf-magnetic field. We introduce the truncated Bose-Einstein distribution function to describe the thermalized distribution of the noncondensed atoms in such a truncated potential [13,16]:

$$\tilde{f}(\mathbf{r},p)=\frac{1}{\exp(\varepsilon_p/k_BT)/\tilde{\xi}(\mathbf{r})-1}\Theta\big(\tilde{A}(\mathbf{r})-\varepsilon_p\big), \tag{1}$$

where $\epsilon_p = p^2/2m$ is the kinetic energy of atoms with momentum p and mass m, T is the temperature, and $\Theta(x)$ is the step function. Hereafter we add a tilde to the notations of the quantities obtained through this truncated distribution function. The function $\tilde{\xi}(\mathbf{r})$ represents the local fugacity at the position $\mathbf{r}$ including the mean-field potential energy: $\tilde{\xi}(\mathbf{r}) = \exp\{[\mu - U(\mathbf{r}) - 2\upsilon\tilde{n}(\mathbf{r})]/k_BT\}$, where μ is the chemical potential, $\upsilon = 4\pi a\hbar^2/m$ is the interaction strength of atoms in proportion to the s-wave scattering length a, and $\tilde{n}(\mathbf{r})$ is the number density of atoms. The step function in Eq. (1) eliminates all the momentum states whose kinetic energies exceed the effective potential depth $\tilde{A}(\mathbf{r}) = \varepsilon_t - U(\mathbf{r}) - 2\upsilon\tilde{n}(\mathbf{r})$, where ε_t is the truncation energy of a magnetic trapping potential determined by the frequency of the applied rf-magnetic field.

The number density of atoms $\tilde{n}(\mathbf{r})$ and the internal energy density $\tilde{e}(\mathbf{r})$ are then evaluated through the truncated distribution function in a self-consistent way:

$$\tilde{n}(\mathbf{r})=\frac{4\pi}{h^3}\int \tilde{f}(\mathbf{r},p)p^2dp, \tag{2}$$

$$\tilde{e}(\mathbf{r})=\frac{4\pi}{h^3}\int \varepsilon_p\tilde{f}(\mathbf{r},p)p^2dp+\upsilon[\tilde{n}(\mathbf{r})]^2+U(\mathbf{r})\tilde{n}(\mathbf{r}). \tag{3}$$

Note that both $\tilde{n}(\mathbf{r})$ and $\tilde{e}(\mathbf{r})$ are the complicated functions of T, μ, ε_t, $U(\mathbf{r})$, and a. Using these density functions, we can straightforwardly calculate the total number of atoms, $\tilde{N} = \int \tilde{n}(\mathbf{r})d\mathbf{r}$, and the total internal energy, $\tilde{E} = \int \tilde{e}(\mathbf{r})d\mathbf{r}$. After the system reaches the critical point T_c of the BEC transition, the number density in the condensed region is given by the sum of a condensate $n_0(\mathbf{r})$ and saturated noncondensed atoms $\tilde{n}_n$ such that $\tilde{n}(\mathbf{r}) = n_0(\mathbf{r}) + \tilde{n}_n$. We approximate $n_0(\mathbf{r})$ using the Thomas-Fermi distribution and evaluate $\tilde{n}_n$ using the truncated Bose-Einstein distribution function under the condition that the local fugacity becomes unity, that is, $\tilde{\xi}(\mathbf{r}) = 1$.

The dynamics of trapped atoms during evaporative cooling is analyzed on the basis of the kinetic theory of a Bose gas [16]. Trapped atoms are removed from the trapping potential by several processes such as evaporation, undesirable collisions, and spilling. Both $\tilde{N}$ and $\tilde{E}$, therefore, become time dependent. The change rates of the total number of atoms and the total internal energy are thus calculated as the sum of the contributions of all these processes:

$$\frac{d\tilde{N}}{dt}=-\int \dot{n}_{\rm ev}(\mathbf{r})d\mathbf{r}-\sum_{s=1}^{3}G_s\int K_s(\mathbf{r})[\tilde{n}(\mathbf{r})]^s d\mathbf{r}+\left(\frac{\partial\tilde{N}}{\partial\varepsilon_t}\right)_{T,\mu}\dot{\varepsilon}_t, \tag{4}$$

$$\frac{d\tilde{E}}{dt}=-\int \dot{e}_{\rm ev}(\mathbf{r})d\mathbf{r}-\sum_{s=1}^{3}G_s\int K_s(\mathbf{r})\tilde{e}(\mathbf{r})[\tilde{n}(\mathbf{r})]^{s-1} d\mathbf{r}+\left(\frac{\partial\tilde{E}}{\partial\varepsilon_t}\right)_{T,\mu}\dot{\varepsilon}_t, \tag{5}$$

where $\dot{n}_{\rm ev}(\mathbf{r})$ and $\dot{e}_{\rm ev}(\mathbf{r})$ denote the evaporation rates of density functions derived from a general collision integral in a Bose gas system and they increase due to the bosonic stimulation below T_c (see Ref. [16]). Parameters G_1, G_2, and G_3 are the decay rate constants of trapped atoms due to background gas collisions, dipolar relaxation, and three-body recombination, respectively. The function $K_s(\mathbf{r})$ represents the correlation function describing the sth order coherence of trapped atoms. We employ the expressions of K_s for an ideal Bose gas system [21–23]. The terms proportional to the change rate of truncation energy, $\dot{\varepsilon}_t = d\varepsilon_t/dt$, describe the contribution of extra atoms that spill over when ε_t is decreased in the forced evaporative cooling [19,20,24].

The time evolution during evaporative cooling is calculated numerically by assuming that the system always stays in quasithermal equilibrium state and is described using the truncated Bose-Einstein distribution function. This quick rethermalization approximation is appropriate for the slow evaporative cooling normally adopted in BEC experiments [13,17].

B. Numerical simulations of evaporative cooling

Our numerical simulations allow us to analyze the whole evaporative cooling process quantitatively without any fitting parameters from the classical regime to the quantum degenerate regime after BEC transition. It is useful to show some calculated results here corresponding to our previous experiments reported in Ref. [18]. We employ the relevant parameters corresponding to our experimental setup. Sodium atoms with $m_F = -1$ in the $F = 1$ state were confined in a cloverleaf-type magnetic trap (MT) characterized by bias field B_0, radial gradient B_r' and axial curvature B_z''. This MT can be modeled

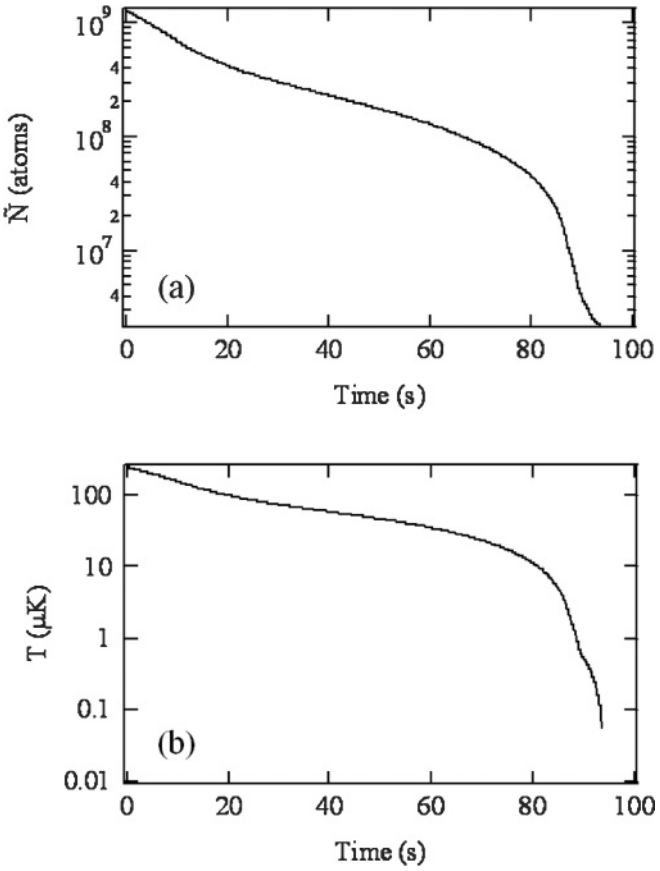

FIG. 1. Time evolution of (a) the total number of trapped atoms $\tilde{N}$ and (b) temperature T during evaporative cooling for 93.7 s.

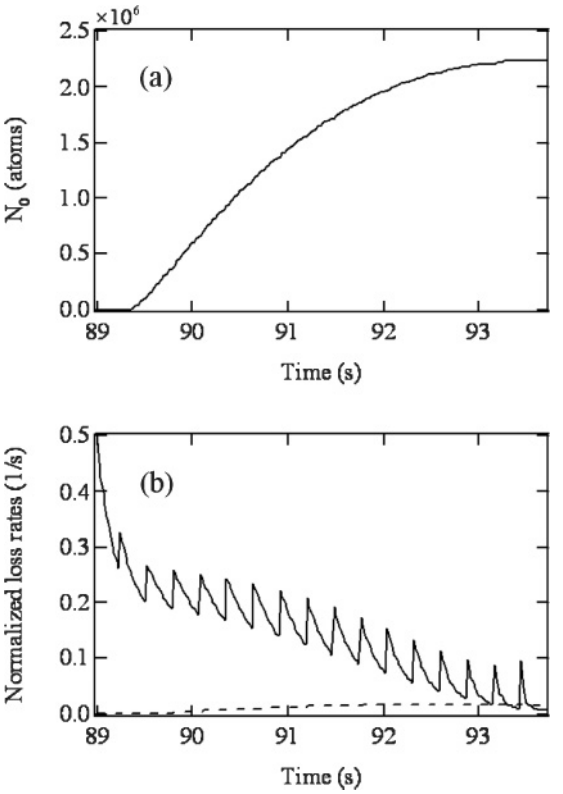

FIG. 2. Time evolution of (a) the number of condensed atoms and (b) the normalized loss rates at the final stage of evaporative cooling. In (b) the solid (dashed) line corresponds to the evaporation (three-body loss) rate.

by a magnetic field of the Ioffe-Pritchard type such that $B(r,z) = \sqrt{(\alpha r)^2 + (\beta z^2 + B_0)^2}$, where $\alpha = \sqrt{B_r'^2 - B_z'' B_0/2}$ and $\beta = B_z''/2$. The values adopted experimentally were $B_0 = 0.11$ mT, $B_r' = 9.8$ mT/cm, and $B_z'' = 15.1$ mT/cm^2 which lead to the trapping frequencies of $\omega_r = 2\pi \times 170$ Hz in the radial direction and $\omega_z = 2\pi \times 21.5$ Hz in the axial direction. The evaporative cooling started from the initial conditions: with $N_{\rm initial} = 1.5\times10^9$ atoms in the MT and at the temperature of $T_{\rm initial} = 250$ μK. The rf frequency was swept stepwise from 33 to 0.69 MHz during about 90 s in a commonly used exponential manner with long step time such as 250 and 280 ms. Furthermore, we set the collisional parameters of sodium atoms in the trapped state of $F = 1$, $m_F = -1$ as follows: s-wave scattering length $a = 2.75$ nm [25], loss rate constant due to collisions with background gas $G_1 = 0.01$ s^{-1} [18], dipolar relaxation $G_2 = 6 \times 10^{-17}$ cm^3 s^{-1} [26], and three-body recombination $G_3 = 6.6\times10^{-30}$ cm^6 s^{-1} [19]. Here we choose both G_2 and G_3 as the values for distinguishable thermal bosons.

In Figs. 1(a) and 1(b) we show the calculated time evolution of the number of trapped atoms $\tilde{N}$ and the temperature T for 93.7 s of evaporative cooling, respectively. Both quantities decrease highly exponentially depending on the sweeping function of rf frequency: $\tilde{N}$ changes from 1.3×10^9 to 2.2×10^6 and T from 250 μK to 56 nK. We find that the system enters the transition point of Bose-Einstein condensation at the time of $t = 89.32$ s, which is consistent with the experimental results shown in Ref. [18]. Figure 2(a) shows the growth of the condensate at the final stage of evaporative cooling. The number of condensed atoms N_0 increases slowly up to 2.2×10^6 over more than 4 s, which also reasonably agrees with the experimental results shown in Ref. [18]. In Fig. 2(b), on the other hand, we plot the time evolution of loss rates normalized by the total number of trapped atoms at each time. The normalized evaporation rate plotted by the solid curve shows the sawtooth time dependence around the BEC transition point due to a rather long time step of rf-field frequency employed experimentally. It is clear that a longer time step significantly lowers the efficiency of evaporative cooling. We also have found that, for this relativity small condensate of sodium, the three-body loss indicated by a dashed line becomes much smaller than evaporation, which is consistent with the fact that any influence of the three-body loss on the condensate growth was not observed experimentally in Ref. [18].

C. Optimization of evaporative cooling

Our numerical simulations can be applied to the optimization of evaporative cooling for achieving high cooling efficiency [19]. As explained in Sec. II A, the time evolution of evaporative cooling intricately depends on various experimental parameters: number of atoms, temperature, MT potential, frequency of applied rf field, undesirable losses of trapped atoms, and so on. Here we focus on the simplest case where only the sweeping function of rf-field frequency is optimized. The cooling trajectory during the evaporative cooling is

optimized approximately by the instantaneous optimization procedure investigated in Ref. [27]. One can determine the optimized cooling trajectory so as to achieve the maximum increase in phase-space density $\tilde{\rho}$ with the smallest decrease in the number of trapped atoms $\tilde{N}$. For the nonuniform atomic gasses trapped in a magnetic potential, the phase-space density is evaluated at the peak position and given by $\tilde{\rho} = \tilde{n}(\mathbf{0})\lambda_{\mathrm{dB}}^3$ with the thermal de Broglie wavelength $\lambda_{\mathrm{dB}} = h/\sqrt{2\pi m k_B T}$. At each time we numerically calculate the optimum truncation energy ε_t^* by maximizing the derivative $\gamma = -d(\ln\tilde{\rho})/d(\ln\tilde{N})$, which describes the efficiency of evaporative cooling [19,27]. The obtained function $\varepsilon_t^*(t)$ corresponds to the optimized sweeping function of rf-field frequency.

In the next section we will show the experimental realization of highly efficient evaporative cooling for sodium atoms. We successfully create a large Bose-Einstein condensate by a rapid sweep of frequency at the final stage of evaporative cooling so as to overcome serious three-body loss, which has been demonstrated for rubidium condensates [17].

III. EXPERIMENTS AND RESULTS

A. Trapping atoms in a magnetic trap

In the present experiment, to increase the number of atoms trapped in the MT, we adopted the spin polarization technique before the magnetic trap and direct catching into a highly compressed clover-leaf trap. Similar to our previous paper [18], we cooled the sodium atomic beam from the oven using σ^+-Zeeman slower and trapped it into a magneto-optical trap (MOT) using the method of dual-operated magneto-optical trap [28], the temporal dark MOT, and the polarization gradient cooling, in turn. The number of trapped atoms in the $F = 1$ state was 1×10^{10} atoms, the density was 1×10^{11} atoms/cm^3, and the temperature was 160 μK. The trapped atoms in the MOT were populated in the three magnetic sublevels with equal distribution, but only atoms in the weak field seeking $m_F = -1$ state can be transferred into the MT. Therefore, before catching into the MT, the spin of the trapped atoms was polarized in the $F = 1, m_F = -1$ state by the spin polarization technique developed by van der Stam *et al.* [29]. After the MOT magnetic field and the trap laser beam were turned off, we first applied the magnetic field of 13 mT along the z axis of the MT for 3 ms using the curvature coils of the cloverleaf coil, 2 ms later, the spin-polarizing beam with σ^- polarization which pumps atoms from the $F = 1$ to $F' = 2$ states, was turned on for 1 ms, and the depumping beam, which depumps atoms in the $F = 2$ state to the $F = 1$ state, was turned on in the last 0.1 ms. The MOT beams were used as the depumping beam.

We prepared a cloverleaf-type magnetic trap with the trap parameters of $B_r' = 10.9$ mT/cm and $B_z'' = 15.1$ mT/cm^2, and $B_0 = 0.13$ mT. These lead to trap frequencies of $\omega_r = 2\pi \times 190$ Hz and $\omega_z = 2\pi \times 21.5$ Hz, which were compressed by 10% more than the previous one [18], but less than half of those of MIT [10]. In our magnetic trap, atoms were loaded directly into the MT with a compressed magnetic field for 1 s without mode matching between the trapping potentials of the MT and MOT, because the transfer efficiency was better than that by the method that was composed of catching atoms into harmonic potential and an adiabatic compression of the potential. The number of atoms trapped into MT with spin polarization was more than twice that without spin polarization. With a careful alignment of the potential between the MT and MOT, the number of atoms trapped in MT increased to $(6.6 \pm 0.1) \times 10^9$ atoms at a temperature of 270 μK and density of 2×10^{11} atoms/cm^3, as given in Table I. The lifetime of atoms remaining in the MT was measured to be 40 s under the present vacuum condition. The trap minimum was evaluated to be 0.70 MHz initially, but it drifted by 6 kHz/s after driving MT with a high current of 240 A.

B. Evaporative cooling

The evaporative cooling process was determined experimentally so as to obtain a maximum increase in phase space density with respect to the decrease in atom number by trial and error. The frequency of the rf-magnetic field was decreased from the initial truncation frequency ν_{initial} to the final frequency ν_{final} by a frequency step $\Delta\nu$ at each time step $\Delta\tau$. At first, the initial truncation frequency was found to be 38 MHz, which corresponds to a trap potential of 1.78 mK. We divided off the rf sweep frequency into eight sections. The time step $\Delta\tau$ is also an important parameter for achieving highly efficient evaporative cooling, as has been discussed in Sec. II B using Fig. 2(b). Here we selected $\Delta\tau$ to be slightly larger than the rethermal equilibrium time, which is

$$t_e = \frac{2.7}{32na^2}\sqrt{\frac{m}{\pi k_B T}}, \tag{6}$$

where n is the density of trapped atoms [9]. Figure 3 shows the experimentally measured t_e values during evaporative cooling. As a result, $\Delta\tau$ was set to be 75 ms for the first section and 50 ms for other six sections, which were one-fifth of the previous $\Delta\tau$ [18]. The truncation parameter of $\eta = h\nu_{\mathrm{rf}}/k_{\mathrm{B}}T$ was selected to be maintained to be more than 6 during the cooling [9]. After trial and error, $\Delta\nu$ and $\Delta\tau$ were determined

TABLE I. Number N, density n, temperature T, and phase space density of ensemble of sodium atoms ρ obtained at different stages in the preparation of ultracold atoms. *Temperature of the phase transition.

Stage	N (atoms)	n (cm^{-3})	T (μK)	ρ
Dual MOT	3×10^{10}	5×10^{10}	1000	8×10^{-8}
Temporal dark MOT	1×10^{10}	2×10^{11}	370	1×10^{-6}
PGC	1×10^{10}	1×10^{11}	160	2×10^{-6}
DMT after spin polarization	6.6×10^9	2×10^{11}	270	3×10^{-6}
Bose condensation	6.4×10^7	8.4×10^{14}	2.2*	$\rho > 2.612$

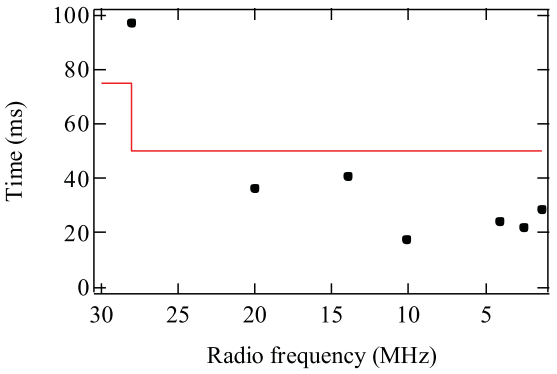

FIG. 3. (Color online) Time step $\Delta\nu$ (solid line) and rethermal equilibrium time (black dot) vs radio frequency.

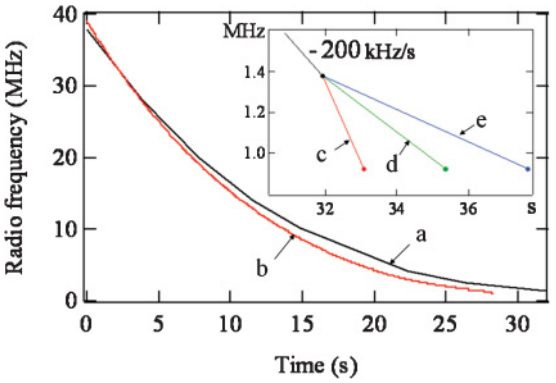

FIG. 4. (Color online) Truncation frequency ν_{rf} as a function of evaporative time. Experiment: black line (a). Optimized simulation: red curve (b). Inset shows three kinds of sweep during the final stage. Red line (c): -400 kHz/s, green line (d): -133 kHz/s, and blue line (e): -80 kHz/s.

for seven sections, as listed in Table II and the phase transition occurred at 1.35 MHz with the shortest evaporative time of 32 s and the temperature of phase transition was 2.2 μK. The total evaporation time till phase transition was shortened to one-third of the previous one [18]. The present rf ramp is shown in Fig. 4.

At the final stage with a density of more than 10^{14} atoms/cm^3, the three-body recombination becomes the dominant loss mechanisms of sodium evaporative cooling. Therefore, the rf frequency was quickly reduced in accordance with the way developed by Mukai and Yamashita in the experiments using rubidium atoms [17]. We employed three different linear rf sweeps with changing rates of -400 (fast), -133 (medium), and -80 kHz/s (slow) at the final stage starting from 1.38 MHz. It should be mentioned here that these linear sweeps sufficiently satisfy the quasistatic condition of forced evaporative cooling [30]. In the fast case, $\Delta\tau$ was further shortened to 25 ms which was half that of the former section. Figure 5 shows the experimentally observed increase in the number of condensed sodium atoms for the three kinds of rf sweep. The growth of condensates strongly depends on the rf sweeps due to a serious influence of three-body loss. With a fast rf sweep, the atoms start to condensate at 32 s and N_0 rapidly increase to its maximum value of 6.4×10^7 in 0.8 s. The absorption images of the Bose-Einstein condensates with 6.4×10^7 atoms measured after an expansion time of 40 ms are shown in Fig. 5. The density of condensates was 8.4×10^{14} atoms/cm^3. On the other hand, with the slow rf sweep, N_0 takes a few second for condensates to reach the maximum value and it seems to be saturated at around 35 s. The maximum N_0 for the fast rf sweep is about twice those for the other two rf sweeps. Therefore, the fast rf sweep during the final stage of evaporative cooling works effectively in obtaining a large N_0 in sodium atoms as same as rubidium atoms. Furthermore, we have successfully achieved highly efficient evaporative cooling by the experimental optimization mentioned above. Note that the overall cooling efficiency such as the ratio of the final number of condensed atoms to the initial number of trapped atoms before evaporative cooling has reached up to 0.97%.

IV. COMPARISON BETWEEN EXPERIMENT AND THEORY

In this section we first examine the efficiency of our present evaporative cooling by comparing cooling trajectories between experiment and theory (Sec. IV A). We then discuss the experimentally observed three-body loss influence on the growth of sodium condensates based on the numerical simulations of evaporative cooling in Sec. IV B. We finally show some theoretical predictions of optimized evaporative cooling for producing further large condensates consisting of more than 10^8 sodium atoms in Sec. IV C.

A. Efficiency of evaporative cooling

As has been explained in Sec. II C, it is possible to optimize a sweeping function of rf-field frequency based on

TABLE II. Experimental parameters of rf sweep used in eight sections for evaporative cooling. ν_{rf}: truncation frequency, $\Delta\nu_{rf}$: frequency step, $\Delta\tau$: time step and t: the time elapsed.

Section	ν_{rf} (MHz)	$\Delta\nu_{rf}$ (kHz)	$\Delta\tau$ (ms)	$\Delta\nu_{rf}/\Delta\tau$ (kHz/s)	t (s)
1	38→28	−200	75	−2666	3.825
2	28→20	−100	50	−2000	7.825
3	20→14	−80	50	−1600	11.575
4	14→10.1	−60	50	−1200	14.825
5	10.1→4.1	−40	50	−800	22.325
6	4.1→2.5	−20	50	−400	26.325
7	2.5→1.35	−10	50	−200	32.075
8 (fast)	1.38→1.04	−10	25	−400	32.775

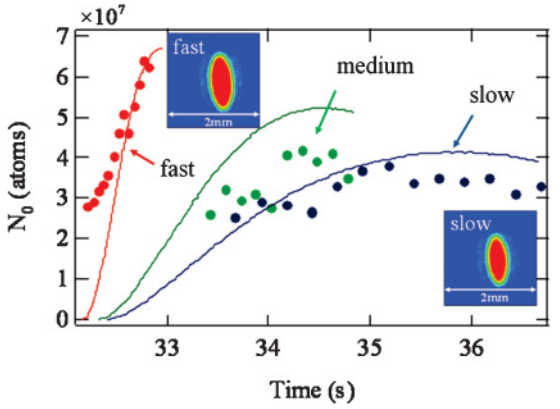

FIG. 5. (Color online) Increase in the number of condensed atoms N_0 for the fast, medium, and slow rf sweeps. Experiment: dots. Simulation: curves. Two absorption images show maximum BECs for fast sweep and slow sweep observed at 40 ms after release from the MT. The numbers of atoms are 6.4×10^7 and 3.8×10^7, respectively.

our numerical simulations. We carry out an optimum simulation corresponding to the present experiment and compare them with the present experimental results. We choose the parameters relevant to our experimental setup: the initial temperature $T_{\text{initial}} = 270\ \mu$K, the initial number of trapped atoms before evaporative cooling $N_{\text{initial}} = 6.7 \times 10^9$, the trap parameters of B_0 [31], B_r', and B_z'', and the drift of bias magnetic field 6 kHz/s as explained in Sec. III B, together with the collisional parameters for sodium in the $F = 1$, $m_F = -1$ trapped state as mentioned in Sec. II B except for $G_1 = 0.025$ s^{-1} derived from the 40-s lifetime of trapped atoms.

The calculated optimum rf sweep is indicated by a red solid curve in Fig. 4 along with the rf ramp obtained experimentally. Both curves are almost the same, although the calculated rf sweep is slightly faster than the experimental one. The experimental optimization of rf sweep is strongly supported by the numerical simulation based on the kinetic theory. In the optimum simulation, the phase transition occurs at 27.6 s and 1.29 MHz and the maximum number of condensed sodium atoms reaches $N_0 = 6.9 \times 10^7$ at 28.3 s. Note that this value is comparable to the number of condensed atoms we obtained experimentally in the case of the fast linear rf sweep.

It is useful to compare the cooling trajectories between experiment and simulation. Figures 6(a) and 6(b), respectively, show the total number of trapped atoms and the temperature during evaporative cooling as a function of applied rf-field frequency. The measured data for both thermodynamic quantities reasonably agree with the theoretical curves suggesting that quasithermal equilibrium assumed in the numerical simulation was realized experimentally during the present evaporative cooling. Next we discuss the cooling efficiency on the basis of the cooling trajectory through phase space. In Fig. 7 we plot the evolution of phase space density during evaporative cooling as a function of the total number of trapped atoms. Here the phase space density is normalized by the critical value of $\rho_c = 2.612$ so that the BEC transition occurs when $\rho/\rho_c = 1$. All the measured data are close to the optimum simulation curve reflecting that very high cooling efficiency has been maintained during the whole evaporative cooling process in

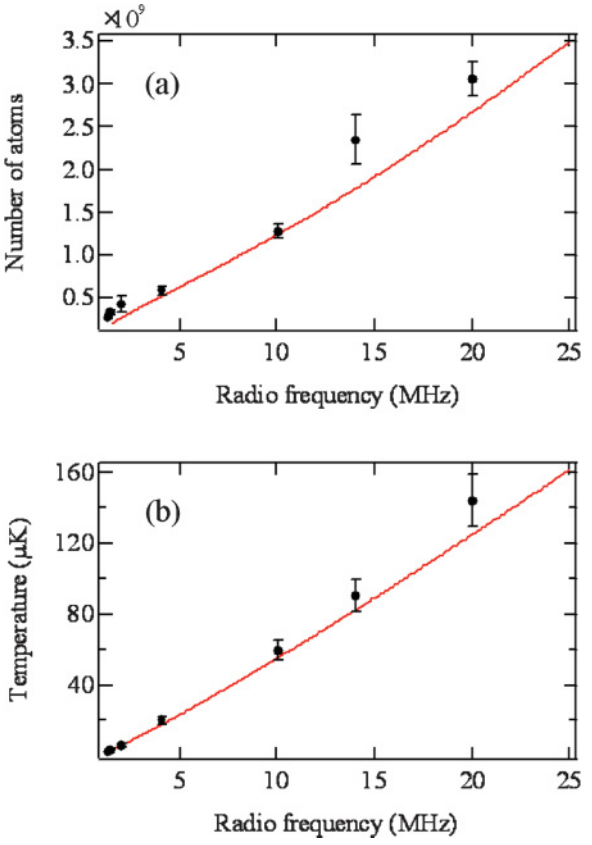

FIG. 6. (Color online) (a) The number of trapped atoms and (b) temperature vs radio frequency. Solid curves are those of simulation.

our experiment. Finally, we compare the truncation parameter η. As shown in Fig. 8, the η value of the optimum simulation is larger than the experimental one. This suggests that our experimental sweep removes more atoms than the optimum simulation during the forced evaporative cooling. However, owing to the finite rethermalization time shown in Fig. 3, the measured smaller η value in our experiment can realize the high cooling efficiency nearly equal to the optimum one obtained by the numerical simulation, as has been confirmed by Fig. 7.

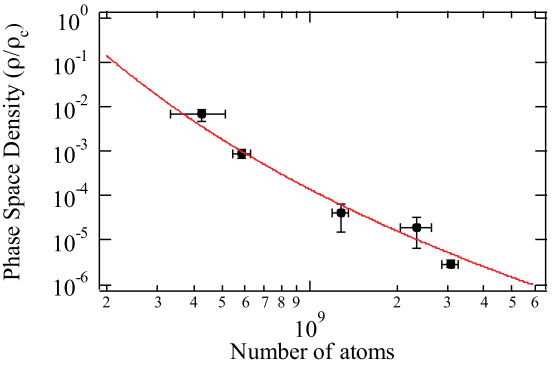

FIG. 7. (Color online) Ratio of the phase space density on $\rho_c = 2.612$ vs the number of atoms trapped in the magnetic trap. Solid curve is simulation.

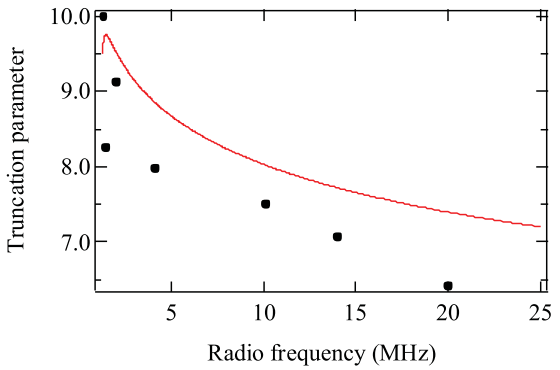

FIG. 8. (Color online) Truncation parameter as a function of radio frequency. Solid curve is simulation.

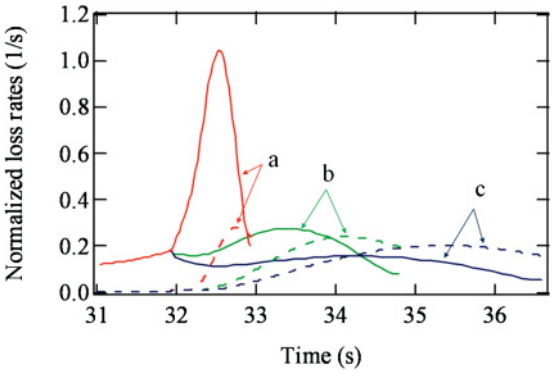

FIG. 9. (Color online) Time dependence of evaporation rates (solid line) and three-body loss rates (dashed line) that are normalized by the total number of trapped atoms at each time. Colors of lines such as red (a), green (b), and blue (c) correspond to the fast, medium, and slow sweeps, respectively. Evaporation rates are averaged out over each step time to eliminate their time dependence of sharp sawtooth shape.

B. Three-body recombination loss

Here we analyze the influence of three-body loss on the growth of sodium condensates observed in Fig. 5. For this purpose we have numerically simulated the present optimized evaporative cooling using both rf sweeps and step times employed experimentally that are summarized in Table II. Other parameters are exactly the same as in the previous subsection.

We show in Fig. 5 the time dependence of N_0 calculated for the three kinds of linear rf sweeps by the corresponding solid lines, together with the experimental results. The condensate growth obtained by the simulation also strongly depends on the changing rates of rf-field frequency. Especially the experimental data for both fast and slow rf sweeps agree quantitatively with the calculations, even though the experimental condensate for the fast rf sweep is generated at the shorter time than the calculation. The maximum N_0 value obtained in the numerical simulation is 6.7×10^7 for the fast rf sweep.

Loss rates calculated numerically provide us with the important information on the dynamics during evaporative cooling [17]. Table III shows various loss rates of trapped atoms at the typical times of three rf sweeps. Figure 9 depicts the time evolution of normalized loss rates of trapped atoms caused by evaporation (solid lines) and three-body recombination (dashed lines) for three rf sweeps. Here we average out the time dependence of evaporation rates over each short step time and eliminate their sharp sawtooth shapes to show the graph more clearly. In comparison with Fig. 2(b) corresponding to relatively small condensates in our previous experiment, we see in Fig. 9 that three-body loss rates become comparable to evaporation rates indicating a significant influence of three-body loss on the condensate growth in the present experiments. With a fast rf sweep, the three-body loss rate is lower than the evaporation rate throughout most of the evaporative cooling process at the final stage. On the other hand, with a medium (slow) rf sweep, the three-body loss rate finally exceeds the evaporation rate at the time of $t = 33.9$ s ($t = 34.2$ s). These two times reasonably agree with the times when the growth of sodium condensate tends to saturate for both medium and slow rf sweeps as shown in Fig. 5.

Evaporation removes energetic atoms from the trap causing cooling effects. In contrast, three-body recombination selectively removes the trapped atoms with low energy from the high density part of the system causing heating effects. The cooling efficiency is therefore determined by the ratio between these two losses. Figure 9 clearly demonstrates that only a fast rf sweep can keep the highly efficient evaporative cooling during condensate growth by overcoming a serious three-body loss, which leads to a large condensate consisting of 6.4×10^7 sodium atoms in our present experiments. On the other hand, the saturation of the number of condensed atoms for a medium (slow) sweep seen in Fig. 5 can be understood by noting that evaporative cooling becomes inefficient due to a three-body loss during condensate growth.

Van der Stam *et al.* reported the collisional opacity for their fully compressed sodium BEC with a density of $6.6 \times 10^{14}/\mathrm{cm}^3$ was 2.2 and the three-body loss coefficient increased by two orders of magnitude due to the effect of

TABLE III. Various loss rates of trapped atoms at the typical times of three rf sweeps. Note that both evaporation and three-body losses are considerably larger than other losses and dominate the condensate growth at the final stage of evaporative cooling as demonstrated in Fig. 9. $\tilde{N}$: Total number of trapped atoms.

Sweep	Time (s)	$\tilde{N}$ (10^7 atoms)	Evaporation (10^7 atoms/s)	Spilling (10^5 atoms/s)	One-body loss (10^6 atoms/s)	Two-body loss (10^5 atoms/s)	Three-body loss (10^7 atoms/s)
Fast	32.7	8.2	6.2	72	2.1	10	2.3
Medium	34	7.5	1.7	9.1	1.9	8.2	1.8
Slow	35	7.0	1.0	3.9	1.7	6.6	1.4

avalanche [32]. On the other hand, Gorlitz *et al*. produced sodium BEC with a density of $5.2 \times 10^{14}/\text{cm}^3$, but they did not observe the effect of avalanche [33]. In our case, the density of condensed atoms is $8.4 \times 10^{14}/\text{cm}^3$ at maximum. We calculated the collisional opacity of the present BECs for three sweeps using Eq. (4) in Ref. [34] and then found that the collisional opacity reached up to 1.2 for the fast sweep, but they were less than 1 for the medium and slow sweep under evaporative cooling. Actually, the number of BEC atoms for medium and slow sweeps grew gradually showing no avalanche effect. In the case of the fast sweep, we note that rf frequency is rapidly decreasing so as to make evaporation largely exceed three-body loss as shown in Fig. 9. In this situation, atoms with high energy can escape from the trap before multiple collisions occur and strong heating caused by three-body loss can be avoided by active evaporation [32]. We reasonably expect that avalanche effects are sufficiently suppressed for the fast sweep, even if the collisional opacity becomes larger than 1. The quantitative agreement between our experimental results and numerical simulations without avalanche effects supports this conclusion as shown in Fig. 5.

C. Optimization for further large condensates

We have seen that our numerical simulations explain the experimental results quantitatively without any fitting parameters. Before concluding this section, it is useful to show some theoretical predictions for achieving further large condensates of sodium atoms with our experimental setup. The improvement of the initial number of trapped atoms is most promising experimentally so that we perform optimum calculations with a larger N_{initial} value such as 1.5×10^{10} [11]. Other parameters except N_{initial} are exactly the same as in Sec. IV A.

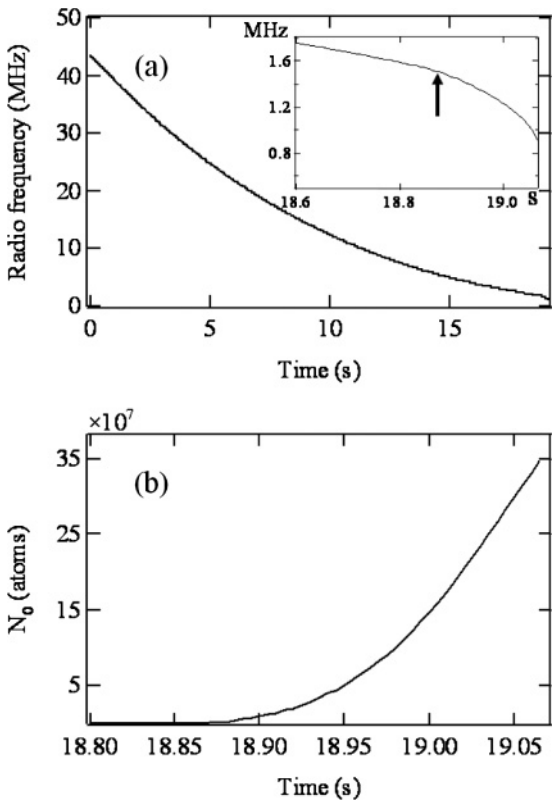

FIG. 10. Optimized evaporative cooling calculated with the initial number of atoms $N_{\text{initial}} = 1.5 \times 10^{10}$: (a) optimized sweep function of rf-field frequency and (b) growth of condensate at the final stage of evaporative cooling. The inset in (a) shows the last part of the optimized sweep of frequency using an expanded scale. The arrow in the inset shows the point at which the BEC transition occurs.

Figure 10(a) shows the optimized sweep of rf-field frequency. When we compare this figure to Fig. 4, both optimized sweeping functions look very similar to each other. However, in Fig. 10(a), the rf sweep starts from a slightly larger frequency of $\nu_{\text{initial}} = 43$ MHz and ends at the shorter time of $t = 19.1$ s. We can qualitatively understand this behavior as a result of higher density of atoms in the magnetic trap when we start evaporative cooling with the larger number of initial atoms. The inset in Fig. 10(a) shows the last part of the optimized rf sweep using an expanded scale. The rf frequency should be swept rapidly around the BEC transition point indicated by the arrow, which can be replaced practically by the fast linear sweep of frequency as experimentally demonstrated by Ref. [17] and the present work.

Figure 10(b), on the other hand, plots the condensate growth in the optimized evaporative cooling with $N_{\text{initial}} = 1.5 \times 10^{10}$. Our simulation predicts a generation of large condensates consisting of more than $N_0 = 3.5 \times 10^8$ sodium atoms after 19.1 s cooling. This value surpasses the largest BEC produced by the Utrecht University group [12]. Furthermore, the overall efficiency of evaporative cooling becomes $N_0/N_{\text{initial}} = 2.3\%$ exceeding our present experimental data. Therefore it can be reasonably expected that both the increase in the initial number of trapped atoms and the corresponding optimized evaporative cooling with a fast linear rf sweep will realize the high cooling efficiency enough for creating large sodium BECs with atoms of the order of 10^8.

V. CONCLUSION

In this paper we have achieved a highly efficient evaporative cooling by optimizing a sweeping function of rf-field frequency experimentally. A large sodium condensate consisting of $N_0 = 6.4 \times 10^7$ atoms has been successfully created by employing a fast linear rf sweep at the final stage of evaporative cooling, starting from the initial number of trapped atoms such as $N_{\text{initial}} = 6.6 \times 10^9$. The overall efficiency of evaporative cooling has reached up to $N_0/N_{\text{initial}} = 0.97\%$. The measured cooling trajectory in our experiment shows a quantitative agreement with the optimum one obtained by the numerical simulations based on the kinetic theory of a Bose gas. The present high cooling efficiency realized experimentally is strongly supported by the theoretical analysis of evaporative cooling.

Furthermore, we have observed a serious influence of three-body loss on the growth of sodium condensates. The final number of condensed sodium atoms strongly depends on the changing rate of rf frequency due to three-body loss. The experimentally measured condensate growth also agrees with the numerical simulations that carefully take account some specific conditions in our experimental setup such a drift of bias magnetic field, finite time steps in frequency sweeps, and so on.

It has been clarified both theoretically and experimentally that a fast linear rf sweep employed at the final stage of evaporative cooling is very effective for creating large sodium condensates by overcoming three-body loss.

We have also shown some numerical simulations that are useful for future experiments. From the calculated results, it seems to be quite possible to realize the highly efficient evaporative cooling enough for producing large condensates having more than 10^8 sodium atoms by simply increasing N_{initial} and the corresponding optimization of evaporative cooling process with a fast linear rf sweep. The experimental demonstration of this theoretical prediction would be an interesting future work.

ACKNOWLEDGMENT

We express our thanks to Dr. Tetsuya Mukai for his beneficial discussions on this study.

[1] M. H. Anderson, J. R. Ensher, M. R. Matthews, C. E. Wieman, and E. A. Cornell, Science **269**, 198 (1995).
[2] K. B. Davis, M.-O. Mewes, M. R. Andrews, N. J. van Druten, D. S. Durfee, D. M. Kurn, and W. Ketterle, Phys. Rev. Lett. **75**, 3969 (1995).
[3] W. Hänsel, P. Hommelhoff, T. W. Hänsch, and J. Reichel, Nature (London) **413**, 498 (2001).
[4] M. Greiner, T. W. Hänsch, and I. Bloch, Nature (London) **419**, 51 (2002).
[5] D. Döring, J. E. Debs, N. P. Robins, C. Figl, P. A. Altin, and J. D. Close, Opt. Express **17**, 20661 (2009).
[6] M. A. Kasevich, Science **298**, 1363 (2002).
[7] H. F. Hess, Phys. Rev. B **34**, 3476 (1986).
[8] K. B. Davis, M.-O. Mewes, M. A. Joffe, M. R. Andrews, and W. Ketterle, Phys. Rev. Lett. **74**, 5202 (1995).
[9] W. Ketterle and N. J. van Druten, Adv. Atom. Mol. Opt. Phys. **37**, 181 (1996).
[10] E. W. Streed, A. P. Chikkatur, T. L. Gustavson, M. Boyd, Y. Torii, D. Schneble, G. K. Campbell, D. E. Pritchard, and W. Ketterle, Rev. Sci. Instrum. **77**, 023106 (2006).
[11] K. M. R. van der Stam, E. D. van Ooijen, R. Meppelink, J. M. Vogels, and P. van der Straten, Rev. Sci. Instrum. **78**, 013102 (2007).
[12] R. Meppelink, S. B. Koller, J. M. Vogels, H. T. C. Stoof, and P. van der Straten, Phys. Rev. Lett. **103**, 265301 (2009).
[13] O. J. Luiten, M. W. Reynolds, and J. T. M. Walraven, Phys. Rev. A **53**, 381 (1996).
[14] P. J. J. Tol, W. Hogervorst, and W. Vassen, Phys. Rev. A **70**, 013404 (2004).
[15] M. Holland, J. Williams, K. Coakley, and J. Cooper, Quantum Semiclass. Opt. **8**, 571 (1996).
[16] M. Yamashita, M. Koashi, and N. Imoto, Phys. Rev. A **59**, 2243 (1999).
[17] T. Mukai and M. Yamashita, Phys. Rev. A **70**, 013615 (2004).
[18] K. Matsui, T. Shobu, Y. Tanaka, H. Nakamatsu, H. Tanaka, and A. Morinaga, J. Phys. Soc. Jpn. **78**, 084301 (2009). In the paper the number of atoms trapped in the MT should be corrected to be 1.3×10^9 and the number of atoms in BEC should be 1.5×10^6.
[19] D. M. Stamper-Kurn, M. R. Andrews, A. P. Chikkatur, S. Inouye, H.-J. Miesner, J. Stenger, and W. Ketterle, Phys. Rev. Lett. **80**, 2027 (1998).
[20] K. Berg-Sørensen, Phys. Rev. A **55**, 1281 (1997); **56**, 3308(E) (1997).
[21] Yu. Kagan, B. V. Svitsunov, and G. V. Shlyapnikov, Pis'ma Zh. EkspTeor. Fiz. **42**, 169 (1985) [JETP Lett. **42**, 209 (1985)].
[22] E. A. Burt, R. W. Ghrist, C. J. Myatt, M. J. Holland, E. A. Cornell, and C. E. Wieman, Phys. Rev. Lett. **79**, 337 (1997).
[23] J. Söding, D. Guéry-Odelin, P. Desbiolles, F. Chevy, H. Inamori, and J. Dalibard, Appl. Phys. B **69**, 257 (1999).
[24] M. Yamashita and T. Mukai, Phys. Rev. A **68**, 063601 (2003).
[25] E. Tiesinga, C. J. Williams, P. S. Julienne, K. M. Jones, P. D. Lett, and W. D. Phillips, J. Res. Natl. Inst. Stand. Technol. **101**, 505 (1996).
[26] H. M. J. M. Boesten, A. J. Moerdijk, and B. J. Verhaar, Phys. Rev. A **54**, R29 (1996).
[27] C. A. Sackett, C. C. Bradley, and R. G. Hulet, Phys. Rev. A **55**, 3797 (1997).
[28] H. Tanaka, H. Imai, K. Furuta, Y. Kato, S. Tashiro, M. Abe, R. Tajima, and A. Morinaga, Jpn. J. Appl. Phys. **46**, L492 (2007).
[29] K. M. van der Stam, A. Kuijk, R. Meppelink, J. M. Vogels, and P. van der Straten, Phys. Rev. A **73**, 063412 (2006).
[30] The time scale of forced evaporative cooling is given by the inverse of the normalized truncation energy changing rate such as $\tau = |\dot{\varepsilon}_t/\varepsilon_t|^{-1}$. The shortest τ in our experiment has been realized during the fast linear rf sweep employed at the final stage of evaporative cooling and is evaluated to be $\tau = 1.5$ s by taking account of the drift of bias magnetic field. Our present evaporative cooling for sodium atoms clearly satisfies the quasistatic condition such that $\tau \gg 2\pi/\omega_r$, $2\pi/\omega_z$, t_e [17].
[31] In numerical simulations, we assume the bias magnetic field of $B_0 = 1.07$ mT that corresponds to the trap minimum of 0.75 MHz. This value is a little bit larger than the experimentally measured one such as 0.70 MHz, which is considered to be within the range of measurement uncertainty.
[32] K. M. R. van der Stam, R. Meppelink, J. M. Vogels, and P. van der Straten, Phys. Rev. A **75**, 031602(R) (2007).
[33] A. Görlitz, T. L. Gustavson, A. E. Leanhardt, R. Löw, A. P. Chikkatur, S. Gupta, S. Inouye, D. E. Pritchard, and W. Ketterle, Phys. Rev. Lett. **90**, 090401 (2003).
[34] J. Schuster, A. Marte, S. Amtage, B. Sang, G. Rempe, and H. C. W. Beijerinck, Phys. Rev. Lett. **87**, 170404 (2001).